Analysis of combustion concepts in a newly designed 2-stroke HSDI compression ignition engine

Jesús Benajes[1], Ricardo Novella[1], Daniela De Lima[1] and Pascal Tribotté[2]

[1]CMT – Motores Térmicos. Universitat Politècnica de València. Camino de Vera s/n, 46022 Valencia, Spain.
Email: rinoro@mot.upv.es

[2]Renault SAS. 1 Avenue du Golf, 78288 Guyancourt, France.
Email: pascal.tribotte@renault.com

Abstract
Two main research paths are being followed to develop compression ignition (CI) engines, the extreme optimization of the conventional diesel combustion (CDC) concept and the development of alternative combustion concepts. The optimization of the CDC concept focuses on exploring the potential of the flexibility provided by the new engine subsystems to control the combustion development in an attempt to improve pollutant emissions and efficiency levels. In the frame of the development of alternative combustion concepts, the Partially Premixed Combustion (PPC) using high volatility and low reactivity fuels, such as gasoline-like fuels with different octane numbers, has been extensively evaluated in 4-stroke engines, confirming its benefits in terms of emissions and efficiency at medium to high loads, but also its critical problems at low loads including difficulties to assure stable ignition and engine efficiency deterioration.

The already confirmed high flexibility of the innovative 2-stroke poppet valves high speed direct injection (HSDI) CI engine under development in terms of air management settings to control the cylinder conditions and affect final combustion environment encouraged the authors to perform a detailed optimization of the CDC concept in an attempt to find the real limits of this engine configuration. Additionally, its compatibility with the PPC concept using a high octane fuel (Research Octane Number 95) with a triple injection strategy for reducing pollutant emissions at medium-to-low load conditions has been evaluated considering also the impact on engine efficiency.

Results at low speed and medium load confirm how the engine configuration provides potential for attaining state-of-the-art emission levels operating with the CDC concept, and how emissions and efficiency can be optimized by adjusting the air management settings without facing any additional trade-off aside from that usual between NO_x and soot. The feasibility of combining this engine configuration with the PPC concept using gasoline as fuel for controlling pollutant emissions has been also corroborated and, with a fine tuned triple injection strategy, engine efficiency even improves compared to that obtained operating with a well optimized CDC concept.

Keywords
Two-stroke engine, gasoline PPC concept, emissions control, engine efficiency

Introduction

Over the last years, engine research efforts are being focused on improving engine efficiency in order to decrease CO_2 emissions and fuel consumption, while fulfilling the increasingly stringent pollutant emissions regulations. In this framework, there is a real need to develop smaller Internal Combustion Engines (ICE) with higher power density. With this motivation, an innovative 2-stroke HSDI CI engine with four poppet valves in the cylinder head is being investigated for a heavily downsized passenger car application, where high power-to-mass ratio is mandatory. The idea behind this new engine concept is to depart from a conventional HSDI diesel 4-stroke engine (1460 cm^3, 4 cylinders) and implement a 2-stroke operation cycle to downsize the engine displacement by a factor of two, obtaining a 2-stroke engine (730 cm^3, 2 cylinders) with equivalent noise, vibration and harshness (NVH) and similar torque response than the base 4-stroke 4 cylinder engine.[1]

Conventional CI engines are well known for their higher thermal efficiency compared to gasoline spark ignition (SI) engines, but the characteristic mixing-controlled combustion stage of the CDC concept still represents an important pollutant source of nitrogen oxides (NO_X)[2-4] and particulate matter emissions.[5, 6] Thus, a very detailed optimization of the CDC concept by adjusting the air management and injection settings is nowadays mandatory to control these emissions keeping the competitive engine efficiency. Many strategies for further improving the mixing process and air utilization during mixing-controlled combustion are still under development, such as ultra-high injection pressure systems[7] combined with micro-hole injector nozzles,[8] multiple or pulsed injection strategies,[9] or new injection rate shaping strategies with novel direct acting piezo-actuated injectors that enables a faster and more precise control of the fuel flow through the injector nozzle compared to conventional electro-hydraulic actuated injectors. [10, 11]

Aside from the efforts to optimize the CDC concept, a relatively new approach known as Partially Premixed Combustion (PPC) concept has been designed to operate CI engines in between fully premixed combustion and fully diffusive combustion concepts, where low emissions can still be attained while retaining control over the combustion timing with the injection event. The injection process is advanced towards the compression stroke to be detached from the combustion event, enabling partial mixing of the mixture to avoid over-rich regions where soot is formed, whereas NO_X emissions are reduced by lowering combustion temperatures by the introduction of large amounts of EGR.[12]

Research work performed by Kalghatgi and co-workers in both large[13, 14] and small[15] single-cylinder engines demonstrated how injecting a fuel with higher resistance to auto-ignition such as a gasoline close to (but before) top dead center (TDC) was suitable for extending mixing times before the onset of combustion. As a result, low engine-out soot and NO_X emissions were obtained in a wider range of engine loads compared to PPC of diesel-like fuels. The authors identified that the mixture stratification on equivalence ratio is mandatory for allowing proper control over the combustion phasing with the injection timing, as for assuring the ignitability of the cylinder charge.

Further research in heavy-duty and light-duty 4-stroke diesel engines operating with PPC concept using gasoline-like fuels and ethanol performed respectively by Wisconsin-Madison University,[16] Lund University[17-22] and more recently by Delphi Corporation,[23-25] confirmed the possibility to implement the PPC concept with very high efficiency, very low NO_X emissions and low soot levels in a wide load operating range. However, the octane number is closely linked to the load range since the fuel ignition properties should be optimized to the given operating condition.[15]

Focusing on the 2-stroke HSDI CI engine configuration under development, the potential of the early-injection Homogeneous Charge Compression Ignition (HCCI) concept using diesel fuel for reducing simultaneously NO_X and soot emissions at low load conditions was experimentally proven.[26] However, the high reactivity of diesel fuel added to the high residual gas fraction (IGR) characteristic of the scavenge loop architecture, made it impossible to attain a properly-phased combustion even operating at low loads with optimized engine settings and hardware, so this combustion concept was discarded.[27] Nevertheless, the high flexibility in terms of air management settings to control the cylinder conditions and affect final combustion environment, also observed operating with CDC concept,[28] encouraged the authors to explore the potential of the PPC concept for pollutant control using a high octane fuel (RON95 gasoline) with a single injection strategy at medium-to-low load conditions. The compatibility of this concept with the 2-stroke configuration in terms of assuring precise control of the onset of combustion and stable PPC operation at low loads was demonstrated.[29]

Recent research work extended the PPC operation to 5 bar and 3 bar of Indicated Mean Effective Pressure (IMEP), when using a single injection strategy with RON95 gasoline. Low NO_X emissions (below 0.4 g/kWh) and zero soot emissions were obtained at these medium/low load conditions, while 98% of combustion efficiency and good combustion stability (covariance of the IMEP under 3%) was retained. However, at higher load (10 bar of IMEP) a transition between premixed and mixing-controlled combustion was observed depending on the particular in-cylinder conditions, and the conventional trade-off between NO_X and soot emissions was recovered.[30]

Thus, present investigation evaluates the strengths and limitations of the 2-stroke poppet valves CI engine under development operating with the CDC concept using diesel fuel and also with the PPC concept using RON95 gasoline. This study was carried out at medium-to-high load (10.4 bar of IMEP) and medium speed (1500 rpm) operating conditions and it includes a detailed analysis of air management and combustion processes together with the exhaust emissions and engine efficiency levels. A design of experiments methodology was used to define the optimum air management conditions operating in CDC, and the available statistical models were used to predefine proper cylinder conditions to assure stable and safe PPC operation. With the aid of CFD calculations, a triple injection strategy was finally selected for improving results operating with PPC, and parametric studies of the main injection timing were experimentally carried out to evaluate the performance of the PPC concept.

Experimental setup

Engine architecture and hardware

Experimental activities were performed in the single-cylinder research version of an innovative Renault engine concept consisting of a 2-cylinder 2-stroke HSDI CI engine with scavenge loop, which is currently under development. Table 1 contains the main engine characteristics.

Table 1. Main engine specifications

Engine type	2-stroke compression ignition
Displacement	365 cm^3 (single-cylinder version)
Bore x stroke	76 mm × 80.5 mm
Connecting rod length	133.75 mm
Compression ratio	17.6:1 (effective CR from 13:1 to 8.8:1)
Number of valves	4 (2 intake & 2 exhaust)
Type of scavenge	Poppet valves with scavenge loop
Valvetrain	Double overhead camshaft with variable valve timing
Nominal intake valve timing (set at VVT=0)	IVO=161.9 cad aTDC IVC=251.6 cad aTDC
Nominal exhaust valve timing (set at VVT=0)	EVO=122.6 cad aTDC EVC=226.9 cad aTDC

CR: compression ratio; VVT: variable valve timing; IVO: intake valve opening; IVC: intake valve closure; EVO: exhaust valve opening; EVC: exhaust valve closure; cad: crank angle; aTDC: after top dead center.

The cylinder head, shown in Figure 1, has four poppet valves with double-overhead camshafts and a staggered roof geometry, specifically designed for baffling the flow of air between the intake and exhaust valves, allowing proper scavenging of the burnt gases while keeping short-circuit losses as low as possible during 2-stroke operation. A hydraulic cam-driven Variable Valve Timing (VVT) system allows delaying intake and exhaust valve timings with a cam phasing authority of +30 degrees from base timing. Then, the effective compression ratio, effective expansion ratio and overlap period between intake and exhaust, can be modified by adjusting the valve timing angles as desired, providing great flexibility to substantially modify air management characteristics. In this research, the key valve timing opening and closure angles were defined at 0.3 mm of valve lift. The definition of the engine architecture, boost system requirements, combustion chamber geometry and scavenging characteristics of this newly designed engine were reported by the authors in previous publications.[1, 31]

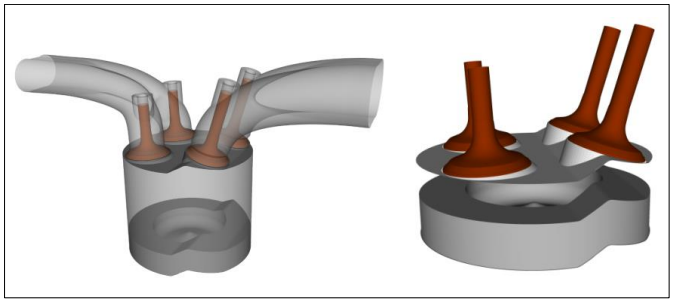

Figure 1. Sketch of the cylinder head designed for the 2-stroke engine architecture (Patent Renault FR2931880).

A conventional piston bowl geometry optimized for diesel combustion was selected for the studies presented in this research, providing a geometric compression ratio of 17.6. Additionally, an optimized 8 hole injection nozzle with 90µm of hole diameter and 155º included spray angle, was used during the tests performed in CDC; while a different nozzle with same flow rate (number of holes and diameter) but slightly lower included angle (148º) was selected for testing the PPC concept. The injection system is a Delphi common rail prototype designed for injecting diesel fuel up to a maximum rail pressure of 1800 bar. Since the injector configuration was fully optimized for CDC concept, a future detailed optimization of the injector operating with the PPC concept is expected to provide a better nozzle configuration in terms of number of holes, holes diameter and/or spray included angle.

Mass flow rate and spray momentum flux were measured in a dedicated test rig[32-35] for the selected injection hardware at analogous test conditions using diesel and gasoline. The injection characteristics are required to be used as inputs of the detailed CFD calculations and also for the combustion analysis from the experimental information.

The injection system main characteristics, as well as the most important fuel properties are detailed in Table 2 for the tests performed with CDC and PPC concepts.

Table 2. Injection system characteristics and most relevant fuel properties

Injection system	Delphi DFI1.5 Common rail HSDI system	
Testing campaign	**CDC tests (diesel fuel)**	**PPC tests (gasoline fuel)**
Injector nozzle	155° AN, 8 holes, 90 µm	148° AN, 8 holes, 90 µm
Maximum allowed injection pressure	1800 bar	1100 bar
Test fuel	Regular fuel pump Diesel	Unleaded gasoline with lubricity additive
Cetane Number	46.6	-
Research Octane Number	-	94.6
H/C ratio	2.06 mol/mol	1.76 mol/mol
O/C ratio	0 mol/mol	0 mol/mol
Oxygen content	<0.5 % (m/m)	<0.17 % (m/m)
Stoichiometric air/fuel ratio (by mass)	14.802	14.37
LHV	42.124 MJ/kg	42.82 MJ/kg
Density (15°C)	843.3 kg/m³	758.1 kg/m³
Kinematic viscosity (40°C)	2.46 cSt	0.44 cSt

HSDI: high speed direct injection; AN: spray included angle; H/C hydrogen/carbon ratio; O/C oxygen/carbon ratio; LHV: lower heating value.

Test cell characteristics

The research single-cylinder engine is assembled into a fully instrumented test cell, equipped with independent water and oil cooling circuits, an external compressor unit for providing compressed air (oil and water-free) and simulate the required boosted conditions, and an additional low pressure EGR system to provide arbitrary levels of cooled EGR even at very high intake pressures. In the 2-stroke configuration with scavenge loop a positive pressure drop between the intake and exhaust ports, denoted as ΔP, is mandatory over the complete range of engine speeds to allow the proper scavenging of the burnt gases and minimize the rate of internal gas recirculation (burnt gases which are not expelled out of the cylinder after the exhaust event). Therefore, the exhaust backpressure is adjusted by a throttle valve after the exhaust settling chamber, allowing precise control of the ΔP across the engine.

Data of O_2, CO, CO_2, HC, NO_X, N_2O and EGR rate is measured with a state-of-the-art HORIBA gas analyzer. Smoke emissions, in filter smoke number (FSN) units, are measured by an AVL 415 Smokemeter. Additionally, a tracer gas method (using methane as a tracer gas) was implemented to experimentally measure the trapping efficiency (or trapping ratio) in each engine test, which is defined as the mass of delivered charge that has been trapped in the cylinder before combustion divided by the mass of delivered charge supplied to the cylinder (fresh air plus EGR). The internal gas recirculation (IGR) ratio is then defined as the fraction of residual gases retained from the previous combustion cycle in the total trapped mass in the cylinder. The IGR ratio and total trapped mass are estimated in each engine test by simplified thermodynamic calculations.

Instantaneous high frequency signals such as cylinder pressure, pressures at the intake and exhaust ports, rail pressure and energizing current of the injector, among others, are sampled with a resolution of 0.2 cad. Cylinder pressure is measured using a piezoelectric sensor, while a different piezorresistive pressure sensor is placed at the cylinder liner close to the bottom dead center (BDC) to reference the piezoelectric sensor signal. The most important global combustion parameters like indicated mean effective pressure (IMEP), maximum cylinder pressure (P_{max}), pressure gradient (dP/da), combustion noise, combustion phasing angles and heat release rate (RoHR); as well as the initial thermodynamic conditions and wall temperatures required for performing the setup of the CFD model, are calculated from the cylinder pressure signal by means of in-house combustion analysis software ("CALMEC").[36, 37]

CFD Model setup

The computational model was built in the CONVERGE CFD platform. Full coupled open and closed cycle computations using the full intake/exhaust and cylinder geometries were carried out since the combustion chamber is non-symmetric. The computational domain at the intake valve closing (IVC) angle is shown in the left plot from Figure 1. The CFD code uses a structured Cartesian grid with base cell size of 3 mm. Three additional grid refinements linked to flow velocity and temperature were performed by means of an adaptive mesh refinement (AMR) as well as a fixed three level refinement within the spray region.

The injection rate profile was generated from the experimental database available after the injector characterization (mass flow rate and spray momentum flux) performed in dedicated test rigs. The diesel-like injection of gasoline is sim-

ulated by the standard Droplet Discrete Model. Gasoline fuel physical properties are defined using iso-octane as surrogate. Spray atomization and break-up are simulated by means of the KH-RT model. Turbulent flow is modeled by means of the RNG k-ε model with wall-functions in order to account for wall heat transfer. Concerning combustion modeling, a direct integration of detailed chemistry approach was used by means of the CONVERGE code and the SAGE solver. Finally, the chemical mechanism of a PRF blend of n-heptane (5%) and iso-octane (95%) has been used in as fuel surrogate after calibrating their respective mass fractions to reproduce the ignition characteristic of the RON95 gasoline.

The setup and validation of the CFD model was performed at the reference case operating with the PPC concept and the three injection strategy. The quality of the model was evaluated by comparing its combustion and emissions results with those obtained experimentally in the engine. Figure 2 compares the CFD and experimental cylinder pressure and RoHR profiles, including also the data related to exhaust emissions. The CFD model performance is considered as suitable for being used along the evaluation of the potential of the PPC concept.

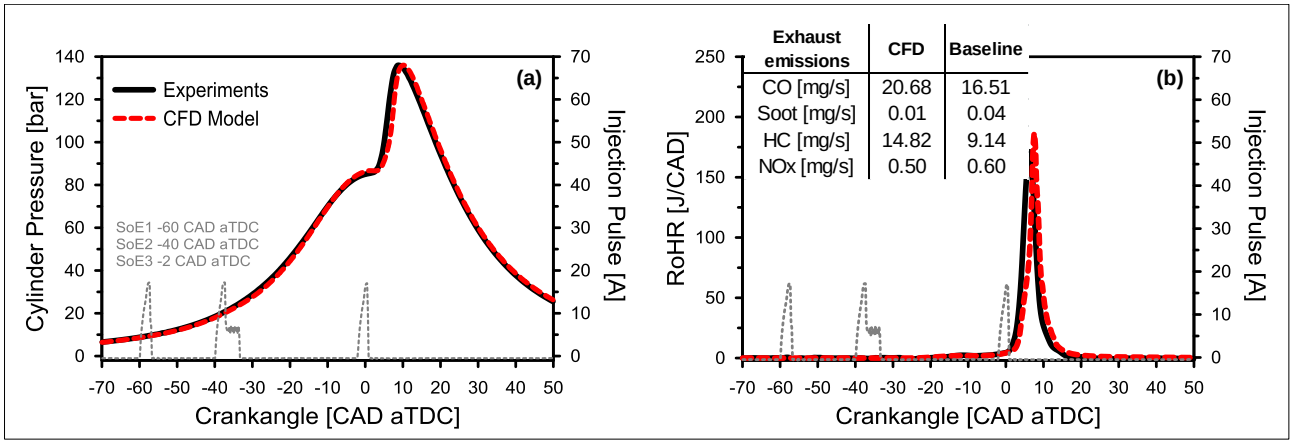

Figure 2. CFD model validation at the reference point operating with the gasoline PPC concept, (a) cylinder pressure and (b) RoHR.

Methodology

The engine operating condition selected for this investigation corresponds with a medium speed (1500 rpm) and medium-to-high load (10.4 bar of IMEP) operating point, and the most relevant experimental conditions as well as the expected targets in terms of exhaust emissions and noise are described in Table 3. The pollutant emissions and noise limits imposed along this initial evaluation of the engine concept corresponds to the Euro 5 levels measured on the equivalent 4-stroke engine in terms of unitary displacement and geometry.

In order to evaluate the performance of this innovative 2-stroke HSDI CI engine with poppet valves configuration in a strictly controlled test environment, it was necessary to define a fast and efficient experimental methodology, which was based on isolating the optimization of the air management parameters from that of the injection parameters. Based on this objective, for the analysis and optimization in CDC, a dedicated Design of Experiments (DoE) technique (Central Composite Design) was selected for easily identifying cause/effect relations of air management parameters on the cylinder conditions, and consequently on combustion process and exhaust emissions. This methodology based on a design of experiments optimization was applied in CDC in two stages. In a first stage, focusing on finding the most suitable cylinder conditions to fulfill the emission limits, especially in terms of NO_X and soot, while keeping low fuel consumption. In a second stage, focusing on further improving engine efficiency (lowest possible fuel consumption) assuming the use of a NO_X after-treatment device (SCR or NO_X trap), and therefore, relaxing the NO_X emissions limits.

The main air management settings selected as factors for the air management DoE are the EGR rate, intake pressure, pressure difference between intake and exhaust (ΔP) and valve overlap duration or intake/exhaust valve timing. The tests were performed keeping a constant injection pressure of 1000 bar and with 2 injection events, one small pilot injection of 2.2 mg/st placed at -19 cad aTDC, and a main injection, for which the injected quantity and timing (SoE_2) are adjusted to maintain a constant value of IMEP of 10.4 bar and a CA50 phased at 6.8 cad aTDC. The ranges of variation for the air management settings included as factors in the DoE, as well as the main injection settings are included in Table 4.

Table 3. Experimental test conditions and emissions and noise limits

Engine speed	1500 rpm
IMEP	10.4 bar
Intake air temperature	35°C
Coolant and oil temperature	90°C
NO_X limit (without NO_X after-treatment)	2.15 mg/s
NO_X limit (with NO_X after-treatment)	10.75 mg/s
HC limit	0.65 mg/s
CO limit	18.65 mg/s
Smoke limit (with DPF)	4.6 FSN
Noise limit	88.3 dB

IMEP: indicated mean effective pressure; DPF: diesel particulate filter

Table 4. Main engine settings and their ranges of variation for the DoE optimization performed in conventional diesel combustion conditions. (a) DoE fulfilling NO_X limit, (b) DoE assuming relaxed NO_X limit.

EGR (%)	P_{int} (bar)	ΔP (bar)	Overlap (cad)	VVT(int,exh) (cad)	P_{rail} (bar)	SoE_1 (cad)	SoE_2 (cad)	Fuel ratio (%)
(a) DoE performed to fulfill NO_X emissions limit (Low NO_X)								
Min: 15 **Max: 25**	**Min: 2.4** **Max: 2.6**	**Min: 0.5** **Max: 0.7**	**Min: 70** **Max: 80**	Min: (13, 18) Max: (13, 28)	1000	-21	-7*	10/90
(b) DoE performed assuming relaxed NO_X limit (High NO_X)								
Min: 0 **Max: 20**	**Min: 2.4** **Max: 2.6**	**Min: 0.45** **Max: 0.85**	73.4	**Min: (0,10)** **Max: (20,30)**	1000	-21	-7*	10/90

DoE: design of experiments; EGR: exhaust gas recirculation; P_{int}: intake pressure; ΔP: pressure difference between intake and exhaust; VVT: variable valve timing; P_{rail}: injection pressure; SoE: start of energizing.
*SoE_2 is adjusted to maintain a constant value of CA50 phased at 6.8 cad aTDC.

For evaluating the potential of the PPC concept with triple injection strategy using gasoline fuel, preliminary air management settings were selected using the mathematical models of the responses obtained with the DoE, in order to find the condition with the highest air trapped mass which allowed introducing the required high EGR rates needed to achieve proper PPC operation with low NO_X and soot emissions, good combustion stability and high efficiency, while simultaneously avoiding operating close to knocking-like combustion conditions. Regarding the three injection strategy selected for PPC operation, first, the range of injection timing was pre-defined with the CFD model by performing parametric studies of the injection timing for each of the three injections; and afterwards, the main trends observed in the calculations were validated with parametric variations of the injection event directly in the engine. The most relevant engine settings chosen for each study is detailed in Table 5.

Finally, the optimum point in CDC fulfilling NO_X and soot targets, the optimum point in CDC with relaxed NO_X limit and the optimum point found in gasoline PPC operation; were selected to be compared in detail. Then, the benefits and limitations of CDC and gasoline PPC concepts will be described to evaluate the compatibility of these concepts with the proposed 2-stroke engine architecture.

Table 5. Main engine settings selected for the parametric optimization of the injection timing performed in gasoline PPC conditions. SoE swept of 2nd injection.

EGR (%)	P_{int} (bar)	ΔP (bar)	Overlap (cad)	VVT(int,exh) (cad)	P_{rail} (bar)	SoE_1 (cad)	SoE_2 (cad)	SoE_3 (cad)	Fuel ratio (%)
43.5	2.75	0.71	78.4	(5,20)	850	**Base: -60**	**Min: -42** **Max: -34**	**Base: -2**	20/64/16

EGR: exhaust gas recirculation; P_{int}: intake pressure; ΔP: difference between intake and exhaust mean pressures; VVT: variable valve timing; P_{rail}: injection pressure; SoE: Start of energizing.

Results & Discussion

Analysis of the Conventional Diesel Combustion (CDC) concept

This analysis will be focused on the first DoE performed in CDC, denoted as (a) in Table 4, designed to fulfill the emissions targets. The DoE methodology allows using statistical models of the responses not only for providing guidelines for optimization, but also for understanding the physical phenomena and existing relations between air management and combustion conditions which then will determine exhaust emissions and engine efficiency.

Table 6 shows the most important statistic quality indicators to check the fit of the quadratic mathematical model for most important measured or calculated responses. The regression coefficient is very close to 1 ("perfect fit") in most of the responses directly measured on the engine, while it slightly decreases (still being acceptable) for the post-processed parameters. Concerning fuel consumption, it was more difficult to assure a perfect fit since the measured range of variation was quite small, around 5%, with some small dispersion of less than 1% on the measured central points of the DoE, but the fit quality was considered as acceptable for further analysis.

Table 6. Statistical analysis of measured & estimated responses

Measured & estimated responses	R^2 (-)	RMSE (-)	PRESS RMSE (-)
Trapping ratio (%)	0.993	0.0033	0.0041
Delivered air flow (fresh air + EGR) (kg/h)	0.997	0.166	0.2
Effective in-cylinder equivalence ratio (-)	0.948	0.0066	0.0077
Oxygen concentration at IVC (%)	0.976	0.00064	0.00066
NO_X emissions (mg/s)	0.990	0.097	0.114
Soot emissions (FSN)	0.964	0.133	0.173
Indicated specific fuel consumption (g/kWh)	0.966	0.394	0.562
Corrected indicated specific fuel consumption (g/kWh)	0.947	0.898	1.131

EGR: exhaust gas recirculation; IVC: intake valve closure; FSN: filtered smoke number; R^2: regression coefficient; RMSE: root mean square error; PRESS RMSE: root mean square prediction error.

Figure 3 shows the relation between trapping ratio and delivered charge mass (fresh air plus EGR) with the two most influential inputs (ΔP and overlap) and also with two key air management parameters, the total mass trapped in the cylinder ($Q_{tot\ trapped}$) and the in-cylinder effective equivalence ratio (ϕ_{eff}). According to this figure, increasing ΔP results in higher Q_{del} levels at the expenses of decreasing trapping ratio by the unavoidably increment of in short-circuit losses due to the cylinder flow path generated by the masking surface. Keeping suitable trapping ratio levels demands to decrease valve overlap, since it directly controls the short-circuited mass flowing from the intake to the exhaust. Intake pressure has slight effects on trapping ratio, but much lower than those of ΔP and valve overlap, while the EGR rate has a very small effect on trapping ratio as expected.

Concerning the IGR ratio, previous studies showed how decreasing trapping efficiency improved the scavenging of burnt gases out of the cylinder, until reaching a practical lower limit, from which decreasing IGR furthermore was not possible.[1] In the present research, the ranges for the air management parameters were pre-selected in advance to assure the lowest percentage of IGR ratio. Within these ranges, the IGR ratio remained approximately constant for all the measured points at levels of around 26 to 27%.

The best combination between trapping ratio and Q_{del} providing the highest $Q_{tot\ trapped}$ is attained with trapping ratio ranging between 66%-68% and Q_{del} around 63-65 kg/h, which corresponds to relatively high ΔP and medium to low values of valve overlap as observed in Figure 3(a) and (b). Accordingly, Figure 3(c) and (d) confirms how the zone with the highest $Q_{tot\ trapped}$, and therefore higher fresh air mass trapped, corresponds to the zone with the lowest values for ϕ_{eff} calculated from the fuel stoichiometric air/fuel ratio, the injected fuel quantity and the usable air available in the trapped charge.

Regarding the combustion process, on the 2-stroke poppet valves architecture it is highly sensitive to the cylinder conditions and then to the air management settings. Thus, the maximum cylinder pressure ranges from 105 bar to 115 bar, and it is phased around 8.4 to 9.6 cad aTDC. This maximum cylinder pressure is determined by $Q_{tot\ trapped}$ and by the cylinder absolute pressure at the IVC, which is controlled by the scavenging process and basically by the valve overlap. The maximum pressure gradient ranges from 3.9 to 4.7 bar/cad, the combustion noise ranges from 86 to 88 dB (below the limit in all cases) and combustion stability traced by the coefficient of variation of IMEP (CoV IMEP) remains below 1.2% in all cases, which are conventional levels operating with the CDC concept.

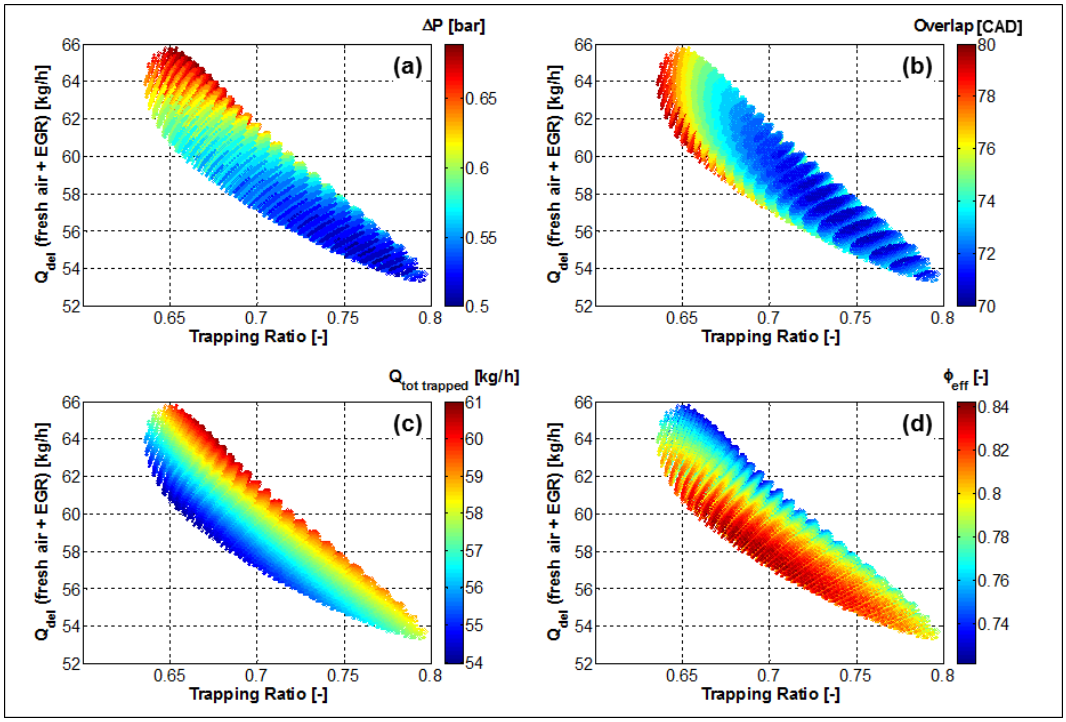

Figure 3. Air management characteristics. (a) Δp, (b) Overlap, (c) total mass trapped and (d) effective in-cylinder equivalence ratio as function of delivered flow and trapping ratio.

From previous discussion, it is evident how the understanding of the relations between the cylinder conditions and the main combustion-related parameters, which are directly linked with the final level of NO_X and soot emissions, is critical in this 2-stroke engine configuration. The maximum adiabatic flame temperature (T_{ad} max) is a suitable tracer on the formation of nitrogen oxides since the thermal mechanisms involved in NO_X formation are chemically controlled and then determined by combustion temperature and oxygen availability at the flame periphery.[3, 4] Furthermore, the late diffusive stage of combustion, between end of injection and end of combustion, is critical for defining the final soot emissions level since the soot oxidation process is substantially slowed down due to the fast decrease of cylinder gas temperature and density. It is known how the soot formed inside the flame is oxidized outside the flame around the stoichiometric zone, by the attack of OH-radicals which are thought to be the major mechanism responsible for soot oxidation in near stoichiometric conditions as in the case of diffusion flames.[2]

Increasing local temperatures at the late stages of combustion and assuring the presence of oxygen is mandatory to increase the rate of formation of OH-radicals and enhance the soot oxidation chemical process.[38, 39] Different authors have used the adiabatic flame temperature at final stages of combustion to describe the late soot oxidation process,[40-42] therefore, the adiabatic temperature calculated at the time where 80% of the fuel has been burnt (T_{ad} 80%MBF) was considered representative of the late soot oxidation temperature.

Figure 4 illustrates the intrinsic relations between the key cylinder conditions, the combustion parameters and the NO_X and Smoke emission levels. Figure 4(a) clearly shows how decreasing YO_2 IVC by increasing EGR rate or by decreasing ΔP and overlap will decrease T_{ad} max, and consequently NO_X formation, due to the dilution effect of the inert exhaust gas inside the combustion chamber. However, as a counterpart, the reduction in fresh air trapped mass will increase ϕ_{eff}. Additionally, the reduction of T_{ad} max by decreasing YO_2 IVC directly leads to an equivalent reduction in T_{ad} 80%MBF, so soot oxidation is worsened as reflected by the increment in smoke emissions observed in Figure 4(b).

It is worth to remark that soot oxidation is also controlled by other parameters besides the temperature at the final stages of combustion. Previous investigations have shown how the spray mixing capacity is proportional to the square root of the product between density and oxygen concentration, if the injection velocity and fuel properties are kept constant.[39, 43] Thus, the mixing capacity calculated at 80% of the MBF (ACT^{-1} 80%MBF), which is crucial for the late soot oxidation process, has been used to trace the spray mixing conditions during the late diffusive combustion stage.

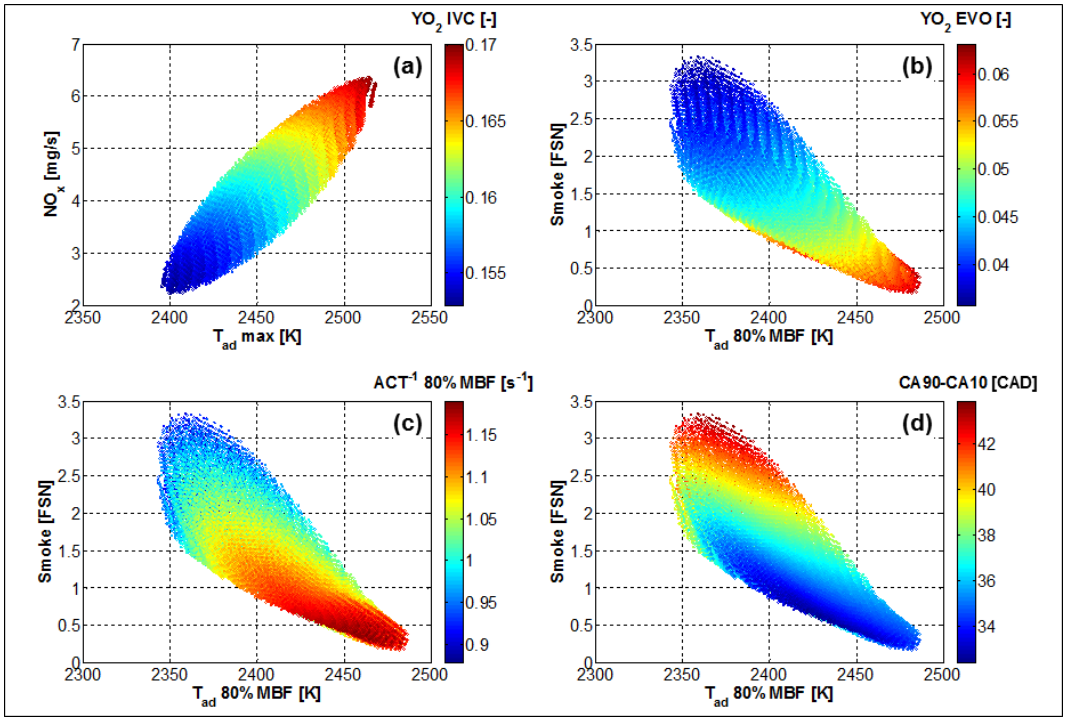

Figure 4. Combustion characteristics. (a) NO_X as function of T_{ad} max and YO_2 IVC, (b) smoke as function of T_{ad} 80%MBF and YO_2 EVO, (c) smoke as function of T_{ad} 80%MBF and ACT^{-1} 80%MBF, (d) smoke as function of T_{ad} 80%MBF and CA90-CA10.

Figure 4(b) and (c) shows how both YO_2 EVO and ACT^{-1} 80%MBF are the key parameters controlling soot oxidation, as reflected in lower smoke emissions in the points with higher fresh air mass trapped (higher YO_2 then lower ϕ_{eff}) and improved mixing conditions. It is worth to recall that the mixing capacity will account for the effects of both YO_2 and gas density, therefore the mixing rate will increase with higher total trapped mass, and also when combustion ends earlier in the cycle (represented with the combustion duration CA90-CA10), so the final stage of combustion occurs at enhanced cylinder conditions, as confirmed by Figure 4(d).

Finally, the smoke-NO_X trade-off will be used for defining the range of variation of the most important emissions along the points of the DoE, and for linking the final emissions levels to the engine fuel consumption. As previously observed in Figure 4, NO_X emissions ranges from 6.5 mg/s to 2.2 mg/s along the points of the DoE and smoke level ranges from 0.15 FSN to 3.18 FSN; while the optimization targets established were 2.15 mg/s and 4.6 FNS respectively. CO emissions sharply increases (up to 22 mg/s) above the required target (18.65 mg/s) when NO_X emissions decreases, following the same trend as soot emissions; while HC emissions are slightly above the target (0.65 mg/s) in most of the points, as shown respectively in Figure 5(a) and (b).

In terms of engine performance, Figure 5(c) illustrates how the indicated fuel consumption is closely related with the emissions levels and therefore with the combustion performance. The points with medium-to-high T_{ad} max and enhanced mixing process have low smoke emissions, medium-to-high NO_X levels and low ISFC, mainly because combustion takes place in a favorable environment for the fuel-energy conversion processes, where the fresh air trapped mass and YO_2 IVC are high and consequently ϕ_{eff} is low. Keeping these cylinder and combustion conditions, it is possible to find the best compromise between NO_X, soot and ISFC; which in Figure 5(c) would correspond to the points with 0.75 FSN of smoke, 3.8 mg/s of NO_X and 190 g/kWh of ISFC. However, Figure 4(a) shows how reducing furthermore YO_2 IVC to decrease T_{ad} max below 2400 K is mandatory to push NO_X emissions below the 2.2 mg/s limit, but both smoke emissions and ISFC increase up to 3 FSN and 200 g/kWh respectively.

Since the two cylinder engine concept presents a double stage supercharging system, with a mechanical volumetric charger set downstream to a WG turbocharger,[1, 31] the ISFC has been corrected ($ISFC_{corr}$) in order to account for the compression work demanded by the air charging devices to achieve the required intake conditions. This correction is useful for estimating qualitatively the increase in BSFC expected at the two cylinder engine with fully assembled air charging system, and to avoid conditions which are not feasible in the two cylinder engine due to very high pressure ratios or extremely high air flow rates. Figure 5(d) illustrates how increasing Q_{del}, mostly by decreasing trapping ratio, causes a sharp increment in $ISFC_{corr}$ despite the almost constant ISFC level. In this case, the additional Q_{del} increases the power demanded by the air management devices, but it is not really used to improve the combustion process and then since most of the flow is directly bypassed. As a result $ISFC_{corr}$ increases because the negligible benefits in ISFC do not compensate the increase in power demanded by the air charging devices, especially by the mechanical supercharger. Therefore, decreasing $ISFC_{corr}$ demands a good combination of initially medium-to-low ISFC with also medium-to-low

Q_{del} to avoid too high power demands of the air management devices. Consequently, the global efficiency of this 2-stroke engine configuration is extremely sensitive to the performance of the turbocharger and supercharger devices, and this should be carefully considered in further stages of development.

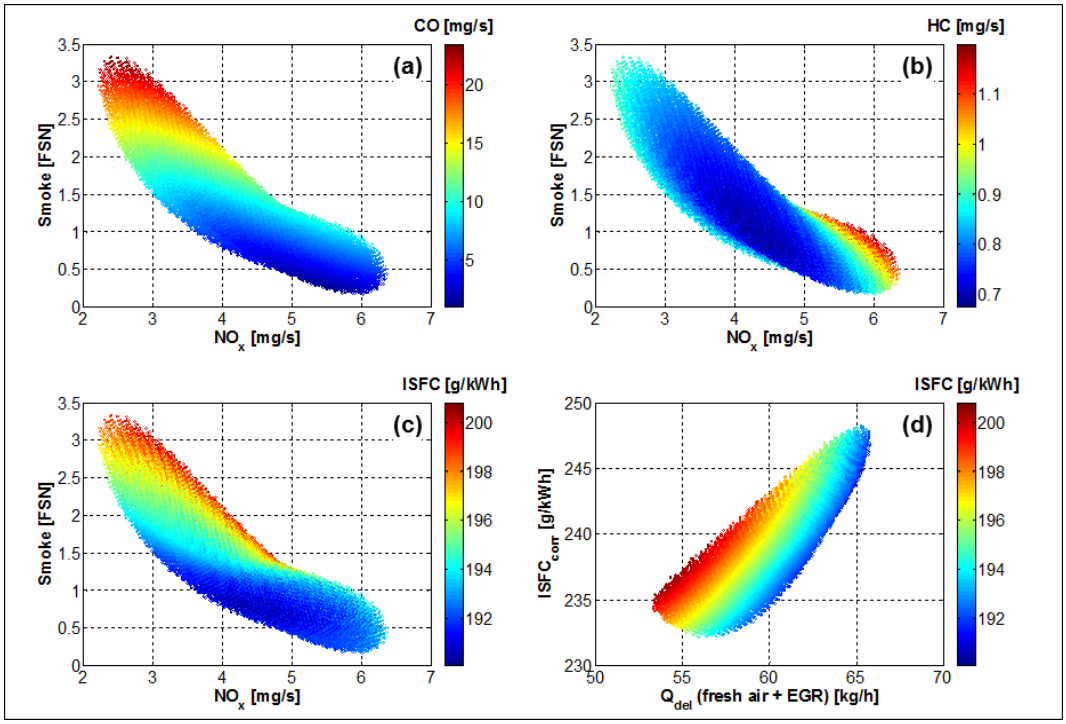

Figure 5. Exhaust emissions and performance. Smoke as function of NO_X and (a) CO emissions, (b) HC emissions and (c) ISFC and (d) $ISFC_{corr}$ as function of delivered flow and ISFC.

This described methodology has been used to analyze the two DoE performed operating with the CDC concept. The first DoE (already discussed) was designed to fulfill the NO_X limit, while the second DoE was designed relaxing the NO_X limit (assuming a SCR or deNO_X after-treatment device) and with slightly different ranges and restrictions for the air management inputs defined with the aim of decreasing fuel consumption as much as possible. Then, the mathematical models of the responses generated by both DoE were also used to select optimum points in terms of air management settings, which comply with the required restrictions in terms of exhaust emissions and fuel consumption.

The proposed optimization methodology was applied in five different operating points which are representative of the NEDC cycle. A summary of the measured optimum points obtained after DoE optimization in terms of emissions and fuel consumption levels is presented in Figure 6, as well as a comparison with the reference 4-stroke engine.

		POINT 1		POINT 3		POINT 4			POINT 5			POINT 6		
		4-stroke K9K	OPT lowNOx	4-stroke K9K	OPT lowNOx	4-stroke K9K	OPT lowNOx	OPT highNOx	4-stroke K9K	OPT lowNOx	OPT highNOx	4-stroke K9K	OPT lowNOx	OPT highNOx
Speed	*rpm*	1250		1500		2000			1500			2500		
imep	*bar*	3.1		5.5		5.8			10.4			15.1		
NOx	*mg/s*	0.45	0.44	0.75	0.73	0.55	3.45	5.29	2.15	2.13	5.91	28.2	21.5	33.1
HC	*mg/s*	0.8	0.54	0.65	0.5	1.35	0.54	0.6	0.65	0.36	0.3	1.3	1.85	1.62
CO	*mg/s*	4.95	3.71	4.4	5.77	9.1	2.98	1.57	18.65	13.02	3.75	3.7	20.68	6.76
FSN	-	1.44	0.33	0.56	0.38	0.73	0.8	0	4.6	2.99	0.41	0.27	1.7	0.54
Bruit	*dB*	84.2	84.48	89.9	89.4	90.2	87.8	89.2	88.3	86.4	87.1	91.5	88.3	88.8
isfc	*g/kWh*	237	208.41	210.25	178	210.7	188.5	183.4	213.6	196.6	186.8	196.37	196.3	192.5
isfc_corr	*g/kWh*	-	226.4	-	215.1	-	211.11	211.22	-	238.7	216.1	-	237.81	237.31

Figure 6. Summary of experimentally measured optimum points found with the DoE methodology at different NEDC representative operating conditions, including the comparison against the reference 4-stroke engine.

Analysis of Partially Premixed Combustion (PPC) using gasoline fuel

The air management settings selected with the aid of the mathematical models generated by the DoE performed in CDC, previously shown in Table 5, correspond to considerably higher EGR rate (43.5%), higher intake pressure and ΔP (2.75 and 0.71 bar) and higher overlap (78.4 cad) compared to CDC. With these settings, the air management parameters correspond to 67% of trapping ratio, 67 kg/h of Q_{del}, 35% of IGR ratio, 0.83 of ϕ_{eff} and 12% of YO_2 IVC, and they were almost constant due to their weak relation with the injection settings. For the reference point (base case) the three injection pattern included a very small 1st injection at SoE_1 -60 cad aTDC, a main 2nd injection where most of the fuel is injected at SoE_2 -40 cad aTDC, and a small 3rd injection close to TDC at SoE_3 -2 cad aTDC.

Regarding the 1st injection, CFD results confirmed how injecting here only the 10% of the total fuel quantity, the liquid fuel impingement onto the cylinder walls is avoided even using a 148º spray included angle injector and relatively high injection pressure of 850 bar. Moreover, results also showed negligible effect of SoE_1 over the combustion onset and RoHR profiles, as well as on exhaust emissions, so 1st injection timing was not experimentally swept.

The effect of SoE_2 over the RoHR is shown in Figure 7 for CFD and experimental results. In the case of CFD simulations, SoE_2 was swept from -34 to -52 cad aTDC, while in the case of experimental results the swept stops at SoE_2 was -42 cad aTDC due to poor combustion stability and misfiring for earlier injection timings. Both CFD and experimental results reveal how the 2nd injection controls both start of combustion (SoC) and phasing. Early SoE_2 increases ignition delay and then the mixing time available for leaning the local equivalence ratios before the start of combustion. As a result, combustion onset & phasing shift towards the expansion stroke as confirmed by CA10 and CA50, shown in Figure 8(a) and (b), while combustion becomes smoother and misfire trending as shows the RoHR. Late SoE_2 closer to TDC decreases ignition delay and mixing time before the SoC, so the local equivalence ratio stratification increases enhancing the reactivity of the mixture. Then, CA10 and CA50 advance towards the TDC, while combustion is faster, shorter and knock-like trending according to the RoHR profile.

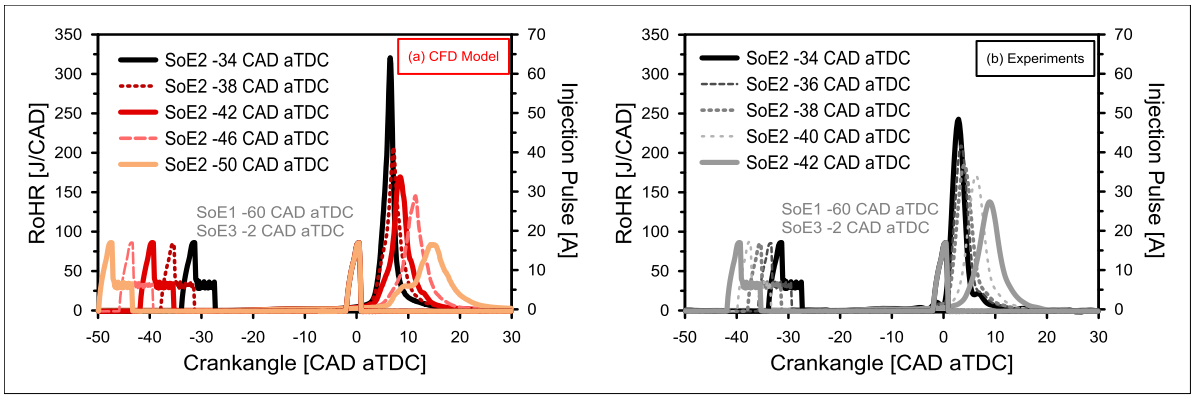

Figure 7. Effect of SoE_2 over the RoHR and injection pulse for (a) CFD and (b) experimental results

Figure 8 (c) to (e) shows how for latest SoE_2 -34 cad aTDC the maximum cylinder pressure is close 150 bar with a very high pressure gradient equal to 22 bar/cad, and noise level over 100 dB, which is caused by the close to knocking fast and short combustion phased near to TDC. For SoE_2 -42 cad aTDC the combustion is smoother, longer and shifted towards the expansion stroke, so P_{max} decrease to 123 bar, dP/da to 10 bar/cad and noise to 93 dB. On the counterpart, retarding combustion phasing to the expansion stroke by advancing SoE_2 brings a consequent increase in the cycle-to-cycle dispersion which cannot be predicted by the CFD simulations, and even when not affecting CoV IMEP *(*which remained between 1% and 1.5%), becomes noticeable when observing the covariance of the maximum cylinder pressure (CoV P_{max}) in Figure 8(f). For SoE_2 earlier than -42 cad aTDC, once the cycle-to-cycle dispersion started to increase and misfire cycles appeared, combustion process could not be sustained properly.

Local conditions were extracted from the CFD simulations in order to further understand the high sensitivity of the combustion process to SoE_2. This analysis was performed at SoE_3 to avoid undesired interferences from the 3rd injection, so the local equivalence ratios distribution generated only by the 1st and 2nd injections will be investigated in detail.

Figure 9 shows a detailed description of the fuel mass at different local equivalence ratios (a) and a summary in form of histogram (b), together with the spatial distribution of the local equivalence ratios in a plane cutting the combustion chamber (c). This analysis includes three different SoE_2 cases: SoE_2 -40 cad a TDC (reference), SoE_2 -34 cad aTDC (latest) and SoE_2 -52 cad aTDC (earliest). Comparing the latest SoE_2 with the reference case, both Figure 9(a) and (b) confirm how higher fuel mass is under the most reactive equivalence ratios due to reduced mixing time and ignition delay. The higher reactivity of the mixture at the start of combustion explains why retarding SoE_2 the combustion rate increases enhancing the knocking trend, as reflected also by the higher maximum pressure gradient.

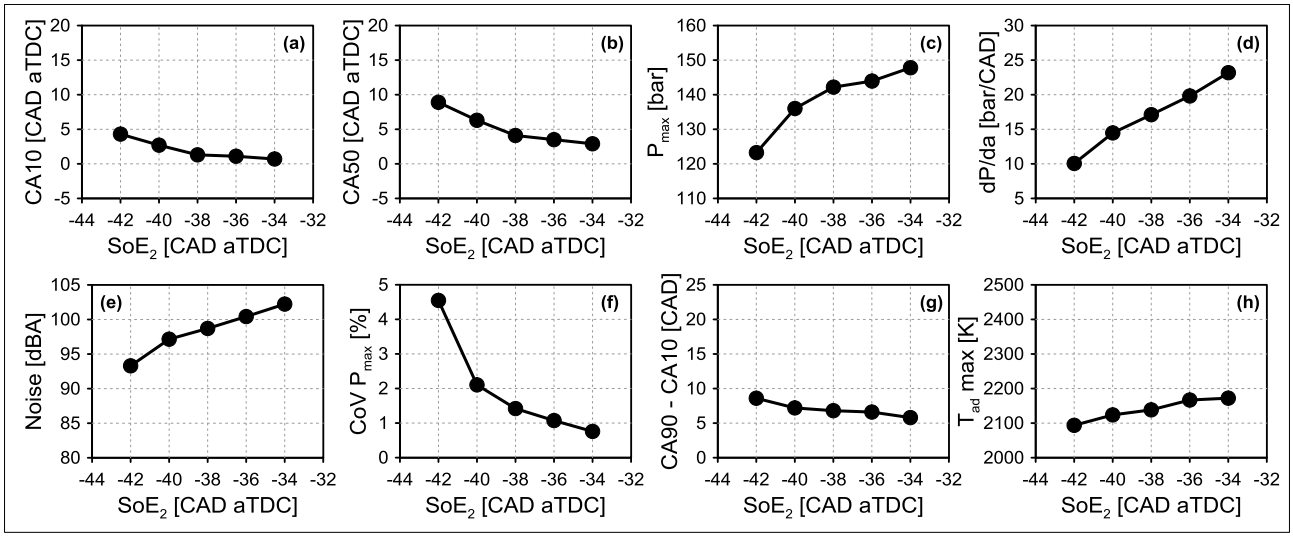

Figure 8. Effect of SoE_2 over combustion characteristics for experimental results. (a) CA10, (b) CA50, (c) maximum cylinder pressure, (d) maximum pressure gradient, (e) noise, (f) covariance of the maximum pressure, (g) CA90-CA10 and (h) maximum adiabatic flame temperature.

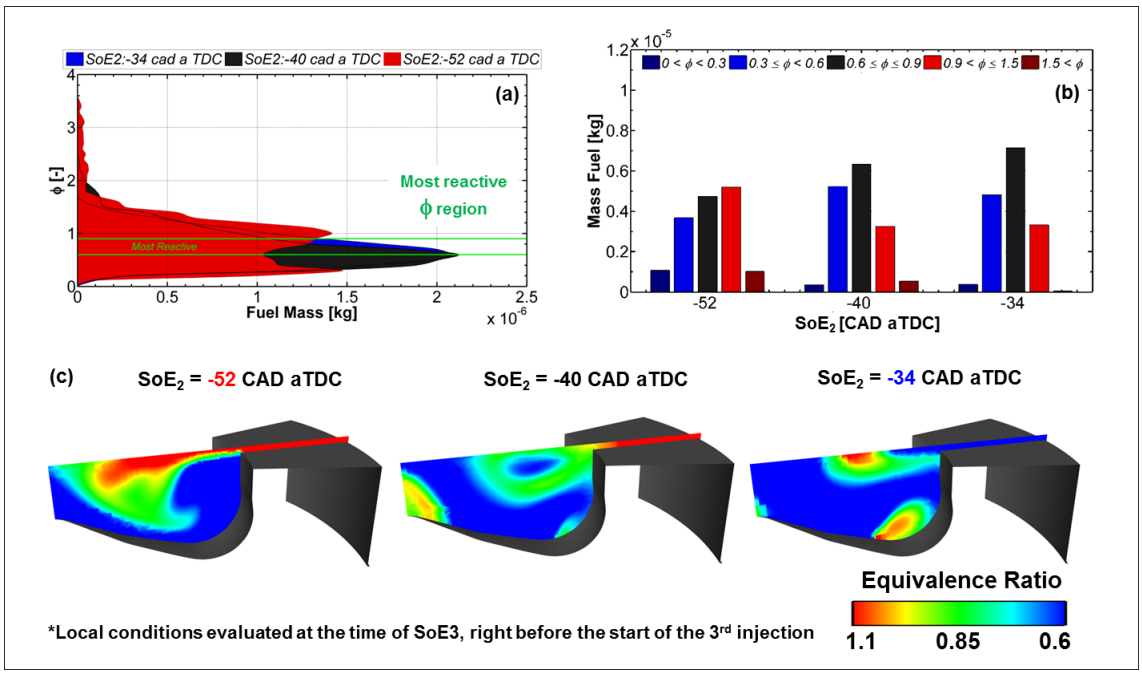

Figure 9. Local conditions evaluated at the time just before injecting the 3rd injection. (a) Equivalence ratio distribution as function of fuel mass, (b) histogram of fuel mass and (c) spatial equivalence ratio distribution for SoE_2 equal to -52, -40 and -34 cad aTDC

Advancing SoE_2 is expected to gradually shift the local equivalence ratio distribution towards leaner and then less reactive conditions due to the extended mixing times as a result of the longer ignition delays. However, according to Figure 9(a) and (b), for the earliest SoE_2 the fuel mass under rich equivalence ratios increases compared to the reference case, while the fuel mass under the most reactive equivalence ratio zone decreases. For the earliest SoE_2 some rich zones (ϕ over 1) are observed in the squish region in Figure 9(c), meaning that the spray is getting split by the bowl lip, directing part of the fuel inside the bowl but also pushing fuel into the squish region where mixing conditions are worsened by the lack of air and lower wall temperature.[44] The fuel trapped in the squish region takes more time to properly mix with air so it remains in rich equivalence ratios by the moment when the 3rd injection starts, and the remaining fuel inside the bowl reaches lean equivalence ratios faster. Therefore, less fuel mass is observed at the most reactive equivalence ratios; as it was previously observed in Figure 9(a). These CFD results explain why it is not possible to test experimentally the points with SoE_2 earlier than -42 cad aTDC due to physical limitations in the current injection hardware given by the use of a conventional wide angle nozzle optimized for diesel combustion. Nevertheless, this opens a possi-

bility for extending the range of operation of the PPC concept in terms of 2nd injection timing by performing a dedicated optimization of the engine hardware in order to extend the window between knock and misfire extreme conditions.

Figure 10 shows the exhaust emissions experimentally obtained sweeping SoE_2. NO_X emissions are substantially decreased (below 1 mg/s) compared with CDC in all points due to the strong reduction in combustion temperature (traced by T_{ad} max), while soot emissions are also lower than the levels observed in CDC when fulfilling the NO_X limit. It is evident how operating with the gasoline PPC concept allows avoiding the NO_X-soot trade-off by decreasing simultaneously both emissions. NO_X emissions decrease for early SoE_2 as the straight effect of the retarded and softened combustion process with lower combustion temperatures. Additionally, smoke also decreases due to the extended ignition delay and thus the mixing time available for the 3rd injection, which is the one acting as the main source of soot emissions by increasing local equivalence ratios at the onset of combustion. However, CO and HC emissions increase.

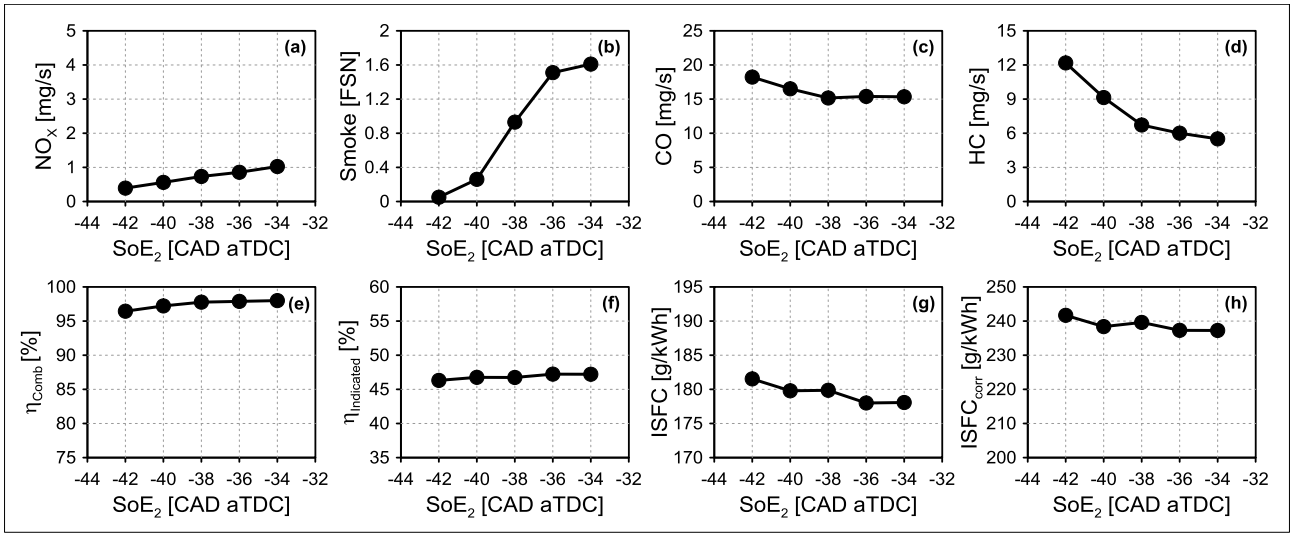

Figure 10. Effect of SoE_2 over exhaust emissions and engine performance. (a) NO_X, (b) Smoke, (c) CO, (d) HC, (e) combustion efficiency, (f) indicated efficiency, (g) ISFC and (h) $ISFC_{corr}$.

Combustion efficiency is relatively lower operating in PPC than in CDC and follows the increase in CO and HC emissions observed in Figure 10(c) and (d), but it remains over 96%-97%, which is in the range or in some cases higher than other results reported in the literature [23]. Finally, indicated efficiency ranges between 46.5% and 47.5% corresponding to ISFC ranging between 181 to 178 g/kWh, so ISFC decreases by 5% compared to the optimum point in CDC with relaxed NO_X limit and 10% compared to the optimum point fulfilling NO_X limit. Despite the clear benefits in ISFC, $ISFC_{corr}$ ranges between 237 and 241 g/kWh and is kept at similar levels than those obtained in CDC with low NO_X limit, due to the increase in mechanical power demanded by the air management devices to achieve the highly demanding equivalence ratio and external EGR rate combinations required to operate in PPC.

Comparative analysis of CDC and gasoline PPC concepts.

The optimum point in CDC fulfilling low NO_X limit, the optimum point in CDC with relaxed NO_X limit, and the optimum point operating with gasoline PPC were selected to be compared in terms exhaust emissions and engine efficiency. Table 7 summarizes the main engine settings, air management characteristics, exhaust emissions and fuel consumption levels experimentally measured.

In the optimum fulfilling low NO_X limit the engine operates with a trapping ratio of 71.4%, Q_{del} of 59.68 kg/h, ϕ_{eff} of 0.83 and YO_2 IVC of 15.19%. The selected in-cylinder conditions allows reaching the required emissions limits, with NO_X emissions of 2.13 mg/s, smoke of 2.99 FSN and CO and HC of 13.02 mg/s and 0.36 mg/s respectively. Finally, at this point an indicated efficiency of 43.47% was obtained, which corresponds with an ISFC of 196.6 g/kWh, and $ISFC_{corr}$ of 238.75 g/kWh if the compression work demanded by the SC/TC devices is considered. Increasing NO_X limit assuming a NO_X after-treatment device, the air management settings can be re-adjusted to favor fuel consumption at the expense of increasing NO_X emissions. The new optimum point defined presents lower EGR, slightly lower intake pressure and ΔP and slightly lower overlap. These new air management settings allowed increasing trapping ratio to 80.7%, decreasing Q_{del} to 50.7 kg/h, decreasing ϕ_{eff} to 0.71 and increase YO_2 IVC to 17.02%. These conditions give higher NO_X (6.41 mg/s), lower smoke and CO emissions (0.53 FSN and 5.09 mg/s) and slightly higher HC emissions (0.5 mg/s). However, operating with lower ϕ_{eff} and improved combustion conditions allowed increasing indicated efficiency

to 45.75%, which correspond with an ISFC of 186.5 g/kWh; while $ISFC_{corr}$ is also decreased to 216.14 due to the reduction in Q_{del} by the new air management settings.

Finally, operating the engine with the PPC concept using RON95 gasoline demands increasing intake pressure, overlap and ΔP to increase Q_{del} and fresh air mass trapped, allowing increasing EGR to 43.5%. In these particular conditions trapping ratio decreases to 68% with IGR of 35%. This combination of fresh air trapped, EGR and IGR allow decreasing YO_2 IVC to 12% while keeping ϕ_{eff} at 0.85. Operating with gasoline PPC was possible decreasing simultaneously NO_X and soot emissions down to 0.5 mg/s and 0.21 FSN, while increasing indicated efficiency to 47%, which is the highest value observed so far in the engine at this load condition. Combustion efficiency keeps at relatively high levels (97.4%) and proper combustion stability is assured with a CoV IMEP of 1.6%. CO emissions increases compared to CDC (15.5 mg/s), but they are kept within the established limit, and HC emissions are considerably higher (8.77 mg/s) compared to CDC probably due to poor injector nozzle matching. Combustion noise noticeably increases when operating in PPC due to the fast and short combustion process generated. Therefore, despite the clear interest of combining the 2-stroke configuration under development with the gasoline PPC concept it is evident how performing a detailed optimization of engine hardware and injection settings to widen the range of operation in terms of SoE_2 is mandatory for further improving these results.

Table 7. Optimum points operating with CDC after performing the DoE air management optimization.

Optimum points measured in CDC and gasoline PPC concept	a) CDC low NO_X limit	b) CDC with relaxed NO_X	Gasoline PPC concept
EGR (%)	26	12	43.5
P_{int} (bar)	2.576	2.5	2.75
ΔP (bar)	0.55	0.45	0.71
Overlap (cad)	76	73.4	78.4
VVT(int,exh) (cad)	(+13,+24)	(+10, +20)	(+5, +20)
Trapping ratio (%)	71.4	80.7	67.9
IGR ratio (%)	26	30	35
Delivered air flow (fresh air + EGR) (kg/h)	59.68	50.7	66.0
Effective In-cylinder equivalence ratio (-)	0.83	0.71	0.85
Oxygen concentration at IVC (%)	15.19	17.02	11.98
Oxygen concentration at EVO (%)	3.90	6.23	4.01
NO_X emissions (mg/s)	2.13	6.41	0.5
Smoke emissions (FSN)	2.99	0.53	0.21
CO emissions (mg/s)	13.02	5.09	15.49
HC emissions (mg/s)	0.36	0.5	8.77
Noise (dB)	86.39	88.0	96.5
Indicated efficiency (%)	43.47	45.75	46.8
ISFC (g/kWh)	196.6	186.5	179.4
$ISFC_{corr}$ (g/kWh)	238.75	216.14	237.5

EGR: exhaust gas recirculation; P_{int}: intake pressure; ΔP: difference between intake and exhaust mean pressures; VVT: variable valve timing; IGR: internal gas recirculation; IVC: intake valve closing; EVO: exhaust valve opening; ISFC: indicated specific fuel consumption; $ISFC_{corr}$: corrected indicated fuel consumption.

Conclusions

A detailed investigation evaluating two combustion concepts, the CDC concept using diesel fuel and the PPC concept using RON95 gasoline, was carried out in the 2-stroke poppet valves HSDI CI engine configuration under development. The most relevant conclusions after the analysis of the results are included below:

Operating with the CDC concept

- For understanding the physical processes linked to 2-stroke engines, it is recommended switching from a particular engine settings to the in-cylinder gas thermodynamic conditions, which later controls the combustion process development, final emissions level and efficiency. The optimum combination of trapping ratio and $Q_{tot\ trapped}$ is obtained with the highest values of ΔP but with the lowest values of valves overlap.
- Low NO_X emissions levels are attainable by reducing YO2 IVC to decrease T_{ad} max along the combustion process, either by introducing EGR or by affecting air management conditions. Reducing T_{ad} max by decreasing YO2 IVC leads to a consequent decrease of the temperatures along the late diffusive combustion stage (T_{ad} 80%MBF), worsening soot oxidation process resulting in higher soot emissions. Nevertheless, increasing the total trapped mass to increase in-cylinder density and enhance the mixing process helps to improve soot oxidation.

- After the optimization process, it was possible to reach the NO_X emissions limit (2.13 mg/s) keeping smoke level also below the target (2.99 FSN) and an engine efficiency of 43.47%. When relaxing the NO_X limit, assuming the use of a NO_X after-treatment device, it is possible to increase indicated efficiency to 45.75% with 0.53 FSN of smoke and 6.41 mg/s of NO_X.
- For low to medium loads & low speed conditions all emission and noise limits were fulfilled even with lower isfc compared to the base 4-stroke engine and important benefits in isfc were observed when relaxing NO_X limits. For high load and medium speed fulfilling soot, CO and HC emissions was not possible since combustion process is compromised due to reduced air flow. However important benefits are expected by improving the acoustic characteristics of the intake and especially exhaust systems.

Operating with the PPC concept

- CFD calculations and experimental results confirmed how the 2nd injection controls both the onset of the combustion as its phasing, whereas the 3rd injection has negligible effect over the start of combustion but controls combustion rate and duration.
- Advancing SoE2 retards the combustion phasing and softens the combustion process decreasing maximum cylinder pressure, pressure rise rate and noise. The earliest SoE2 is limited by the appearance of misfire cycles, which are linked to the interaction between the spray and the piston bowl, so the earliest SoE2 is constrained by the need of avoiding directing the spray towards the squish region. The latest SoE2 is limited by the onset of knocking combustion, which is promoted by the reduced mixing time thus higher reactivity at the start of combustion.
- By properly phasing SoE2 it is possible to decrease simultaneously NO_X and soot (0.5 mg/s and 0.2 FSN respectively), while combustion efficiency is kept in 97.4% and indicated efficiency increases to 46.8%.

The final comparison between the general results provided by both combustion concepts confirms the benefits of the PPC concept in terms of NO_X and soot emissions control even improving by 5% to 10% the indicated efficiency. Results also corroborate the key drawback of the PPC concept related to the increment in maximum pressure gradient and noise level, which is very difficult to control due to the intrinsic fast combustion process generated by this concept. Therefore, a detailed optimization of engine hardware to optimize its compatibility with this combustion concept is expected to allow even further improvements.

Acknowledgments

This research has been partially sponsored by the European Union in framework of the POWERFUL project, FP7/2007-2013, theme 7, sustainable surface transport, grant agreement No. SCP8-GA-2009-234032.
The authors want to express their gratitude to CONVERGENT SCIENCE Inc. and IGNITE3D Engineering GmbH for their kind support for performing the CFD calculations using CONVERGE software.

References

1. Tribotte P, Ravet F, Dugue V, et al. Two Strokes Diesel Engine - Promising Solution to Reduce CO2 Emissions. *Procedia - Social and Behavioral Sciences*. 2012; 48: 2295-314.
2. Dec JE. A Conceptual Model of DI Diesel Combustion Based on Laser-Sheet Imaging. SAE paper 970873, 1997.
3. Dec JE and Canaan RE. PLIF Imaging of NO Formation in a DI Diesel Engine. SAE paper 980147, 1998.
4. Kitamura Y, Mohammadi A, Ishiyama T and Shioji M. Fundamental Investigation of NOx Formation in Diesel Combustion Under Supercharged and EGR Conditions. SAE paper 2005-01-0364, 2005.
5. Flynn PF, Durrett RP, Hunter GL, et al. Diesel combustion: An integrated view combining laser diagnostics, chemical kinetics, and empirical validation. SAE paper 1999-01-0509, 1999.
6. Xu Y and Lee C-fF. Investigation of Soot Formation in Diesel Combustion Using Forward Illumination Light Extinction (FILE) Technique. SAE paper 2004-01-1411, 2004.
7. Meek GA, Williams R, Thornton D, Knapp P and Cosser S. F2E - Ultra High Pressure Distributed Pump Common Rail System. SAE paper 2014-01-1440, 2014.
8. Wang X, Huang Z, Zhang W, Kuti OA and Nishida K. Effects of ultra-high injection pressure and micro-hole nozzle on flame structure and soot formation of impinging diesel spray. *Appl Energy*. 2011; 88: 1620-8.
9. Graham MS, Crossley S, Harcombe T, Keeler N and Williams T. Beyond Euro VI - Development of A Next Generation Fuel Injector for Commercial Vehicles. SAE paper 2014-01-1435, 2014.
10. Payri R, Gimeno J, Viera JP and Plazas AH. Needle lift profile influence on the vapor phase penetration for a prototype diesel direct acting piezoelectric injector. *Fuel*. 2013; 113: 257-65.
11. Macian V, Payri R, Ruiz S, Bardi M and Plazas AH. Experimental study of the relationship between injection rate shape and Diesel ignition using a novel piezo-actuated direct-acting injector. *Appl Energy*. 2014; 118: 100-13.
12. Okude K, Mori K, Shiino S and Moriya T. Premixed Compression Ignition (PCI) Combustion for Simultaneous Reduction of NOx and soot in Diesel Engine. SAE paper 2004-01-1907, 2004.

13. Kalghatgi GT, Risberg P and Ångström H. Advantages of Fuels with High Resistance to Auto-ignition in Late-injection, Low-temperature, Compression Ignition Combustion. SAE paper 2006-01-3385, 2006.
14. Kalghatgi G, Risberg P and Ångström H. Partially Pre-Mixed Auto-Ignition of Gasoline to Attain Low Smoke and Low NOx at High Load in a Compression Ignition Engine and Comparison with a Diesel Fuel. SAE paper 2007-01-0006, 2007.
15. Hildingsson L, Kalghatgi G, Tait N, Johansson B and Harrison A. Fuel Octane Effects in the Partially Premixed Combustion Regime in Compression Ignition Engines. SAE paper 2009-01-2648, 2009.
16. Hanson R, Splitter D and Reitz R. Operating a Heavy-Duty Direct-Injection Compression-Ignition Engine with Gasoline for Low Emissions. SAE paper 2009-01-1442, 2009.
17. Manente V, Johansson B, Tunestal P and Cannella W. Effects of Different Type of Gasoline Fuels on Heavy Duty Partially Premixed Combustion. *SAE Int J Engines*. 2010; 2: 71-88.
18. Manente V, Tunestal P and Johansson B. Effects of Ethanol and Different Type of Gasoline Fuels on Partially Premixed Combustion from Low to High Load. SAE paper 2010-01-0871, 2010.
19. Lewander M, Johansson B and Tunestål P. Investigation and Comparison of Multi Cylinder Partially Premixed Combustion Characteristics for Diesel and Gasoline Fuels. SAE paper 2011-01-1811, 2011.
20. Solaka H, Aronsson U, Tuner M and Johansson B. Investigation of Partially Premixed Combustion Characteristics in Low Load Range with Regards to Fuel Octane Number in a Light-Duty Diesel Engine. SAE paper 2012-01-0684, 2012.
21. Borgqvist P, Tunestal P and Johansson B. Gasoline Partially Premixed Combustion in a Light Duty Engine at Low Load and Idle Operating Conditions. SAE paper 2012-01-0687, 2012.
22. Kaiadi M, Johansson B, Lundgren M and Gaynor JA. Sensitivity Analysis Study on Ethanol Partially Premixed Combustion. *SAE Int J Engines*. 2013; 6.
23. Sellnau MC, Sinnamon J, Hoyer K and Husted H. Full-Time Gasoline Direct-Injection Compression Ignition (GDCI) for High Efficiency and Low NOx and PM. *SAE Int J Engines*. 2012; 5.
24. Sellnau MC, Sinnamon J, Hoyer K, Kim J, Cavotta M and Husted H. Part-Load Operation of Gasoline Direct-Injection Compression Ignition (GDCI) Engine. SAE paper 2013-01-0272, 2013.
25. Sellnau M, Sinnamon J, Hoyer K and Husted H. Gasoline Direct Injection Compression Ignition (GDCI) - Diesel-like Efficiency with Low CO2 Emissions. SAE paper 2011-01-1386, 2011.
26. Benajes J, Novella R, De Lima D, Dugue V and Quechon N. The potential of highly premixed combustion for pollutant control in an automotive two-stroke HSDI diesel engine. SAE paper 2012-01-1104, 2012.
27. Benajes J, Novella R, De Lima D, Quechon N and Obernesser P. Implementation of the early injection highly premixed combustion concept in a two-stroke HSDI engine. SAE paper, 2012.
28. Benajes J, Novella R, De Lima D, et al. Analysis of the combustion process, pollutant emissions and efficiency of an innovative 2-stroke HSDI engine designed for automotive applications. *Appl Therm Eng*. 2013; 58: 181-93.
29. Benajes J, Molina S, Novella R and De Lima D. Implementation of the Partially Premixed Combustion concept in a 2-stroke HSDI diesel engine fueled with gasoline. *Appl Energy*. 2014; 122: 94-111.
30. Benajes J, Novella R, Martín J and De Lima D. Analysis of the Load Effect on the Partially Premixed Combustion Concept in a 2-Stroke HSDI Diesel Engine Fueled with Conventional Gasoline. SAE paper 2014-01-1291, 2014.
31. Pohorelsky L, Brynych P, Macek J, et al. Air System Conception for a Downsized Two-Stroke Diesel Engine. SAE paper 2012-01-0831, 2012.
32. Payri R, Salvador FJ, Gimeno J and Novella R. Flow regime effects on non-cavitating injection nozzles over spray behavior. *Int J Heat Fluid Flow*. 2011; 32: 273-84.
33. Payri R, Salvador FJ, Gimeno J and Bracho G. A new methodology for correcting the signal cumulative phenomenon on injection rate measurements. *Exp Tech*. 2008; 32: 46-9.
34. Payri R, García JM, Salvador F and Gimeno J. Using spray momentum flux measurements to understand the influence of diesel nozzle geometry on spray characteristics. *Fuel*. 2005; 84: 551-61.
35. Payri R, García A, Domenech V, Durrett R and Plazas AH. An experimental study of gasoline effects on injection rate, momentum flux and spray characteristics using a common rail diesel injection system. *Fuel*. 2012; 97: 390-9.
36. Payri F, Molina S, Martín J and Armas O. Influence of measurement errors and estimated parameters on combustion diagnosis. *Appl Therm Eng*. 2006; 26: 226-36.
37. Lapuerta M, Armas O and Hernández J. Diagnostic of D.I. Diesel Combustion from In-Cylinder Pressure Signal by Estimation of Mean Thermodynamic Properties of the Gas. *Appl Therm Eng*. 1999; 19: 513-29.
38. Tree DR and Svensson KI. Soot processes in compression ignition engines. *Prog Energy Combust Sci*. 2007; 33: 272-309.
39. Benajes J, Novella R, García A and Arthozoul S. The role of in-cylinder gas density and oxygen concentration on late spray mixing and soot oxidation processes. *Energy*. 2011; 36: 1599-611.
40. Benajes J, García-Oliver JM, Novella R and Kolodziej C. Increased particle emissions from early fuel injection timing Diesel low temperature combustion. *Fuel*. 2012; 94: 184-90.
41. Payri F, Benajes J, Novella R and Kolodziej C. Effect of Intake Oxygen Concentration on Particle Size Distribution Measurements from Diesel Low Temperature Combustion. SAE paper 2011-01-1355, 2011.

42. Benajes J, Novella R, Arthozoul S and Kolodziej C. Particle Size Distribution Measurements from Early to Late Injection Timing Low Temperature Combustion in a Heavy Duty Diesel Engine. SAE paper 2010-01-1121, 2010.
43. Arrègle J, López JJ, García JM and Fenollosa C. Development of a zero-dimensional Diesel combustion model. Part 1: Analysis of the quasi-steady diffusion combustion phase. *Appl Therm Eng*. 2003; 23: 1301-17.
44. Musculus MPB, Miles PC and Pickett LM. Conceptual models for partially premixed low-temperature diesel combustion. *Prog Energy Combust Sci*. 2013; 39: 246-83.

Notation

ACT^{-1} 80%MBF	Gas mixing capacity at 80% of the mass burnt fraction
ΔP	Pressure drop between the intake and the exhaust
ϕ_{eff}	In-cylinder equivalence ratio
$ISFC_{corr}$	Corrected indicated specific fuel consumption
P_{int}	Absolute mean intake pressure
P_{max}	Maximum cylinder pressure
Q_{del}	Delivered flow rate (fresh air flow + EGR)
$Q_{tot\ trapped}$	Total trapped flow rate (trapped fresh air + trapped EGR + IGR)
SoE	Start of energizing current of the injector
T_{ad} max	Maximum adiabatic flame temperature
T_{ad} 80%MBF	Adiabatic flame temperature at 80% of the mass burnt fraction
VVT(int, exh)	Variable Valve Timing positions (intake, exhaust)
YO2 IVC / EVO	Oxygen concentration at the intake valve closing / exhaust valve opening